PCIM´88 Conference, Tokyo, December 8-10, 1988

ANALYSIS OF THE CLOSED-LOOP CONTROL BEHAVIOR OF A BIDIRECTIONAL HIGH-FREQUENCY DC-DC-CONVERTER

Felix A. HIMMELSTOSS, Johann W. KOLAR and Franz C. ZACH

Technical University of Vienna - Power Electronics Section
Gusshausstrasse 27-29, A - 1040 Vienna, AUSTRIA

A B S T R A C T

A new system for DC-DC power conversion based on a buck-boost converter topology is presented which makes power flow in both directions possible. The possibility of bidirectional power flow will increase the system dynamics and is also useful for certain applications, such as uninterruptable power supplies (UPS) etc. The structure is compared with the well known unidirectional buck-boost converter. Starting from a structure diagram the closed loop control is treated based on simulation using duty cycle averaging. The closed-loop behavior of the bidirectional converter is analyzed; root locus and bode-diagram are shown. The design of a controller is shown for an example.

1. INTRODUCTION

Unidirectional converters in their basic configuration are characterized by an asymmetrical structure regarding their topology and/or regarding their controllability. Switching instants and conduction intervals of the diodes on the secondary are - dependent on the converter topology (buck or boost converters etc.) - determined indirectly by changing the switching status of the power transistor on the primary.

An intrinsic limitation of this concept is given by the direction of current and energy flow (first quadrant of the current-voltage phase plane) which is determined by the direction of the electric valves.

Bidirectional power flow between constant voltage (current) sources requires replacement of the unidirectional power semiconductor devices by an antiparallel combination of a directly (power transistor) and an indirectly (diode) controllable electrical valve. This results in a unidirectionally controllable power semiconducter. However, this requires fixed voltage polarity, equivalent to restriction to the first and second quadrant of the current-voltage plane.

The application of this general concept to a buck-boost converter structure leads to a topology with a remarkably simple topology.

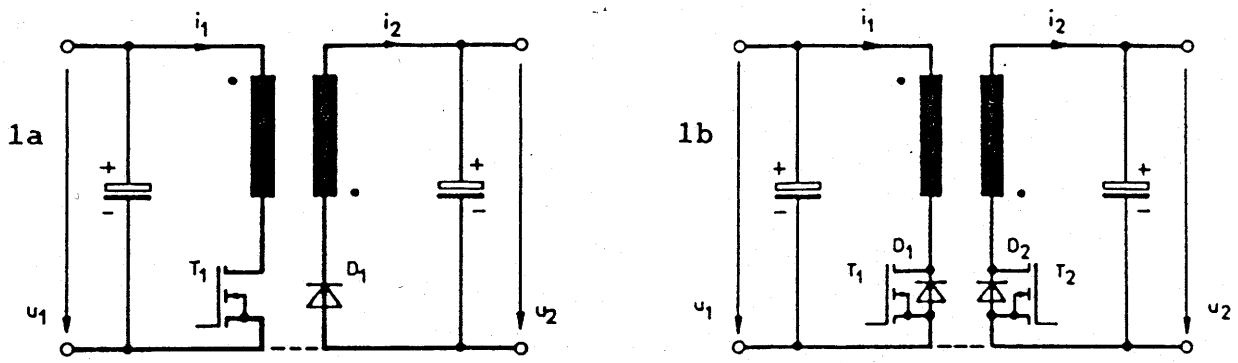

Fig.1 a) unidirectional buck-boost converter
b) bidirectional buck-boost converter

There is only one magnetic device necessary; see Fig.1 where this topology is compared to that of the conventional unidirectional buck-boost converter.

The stationary system condition is characterized by a time constant average energy content of the primary and secondary electrical and magnetic energy storage devices. This equilibrium between energy input and output corresponds to a duty ratio defined only by the voltage ratios (and turn ratios) of primary and secondary independent of the energy flow direction. This is shown in the following. Idealized components are assumed and the push-pull control of T_1 and T_2 as indicated in Fig.2. Vice versa by giving a duty ratio (for stationary, i.e. equilibrium operation) the voltage ratio of the converter can be varied to a large extent.

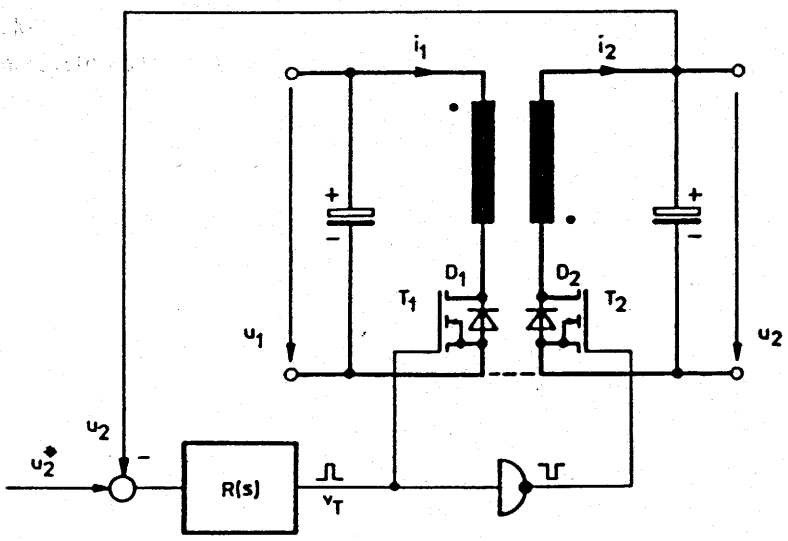

Fig.2 Bidirectional converter with push-pull control

2. SYSTEM DESCRIPTION AND COMPARISON OF UNIDIRECTIONAL AND BIDIRECTIONAL BOOST CONVERTER

Continuous operation is given if the transistor on the primary is turned on again before i_{D2} reaches zero (Fig.3).

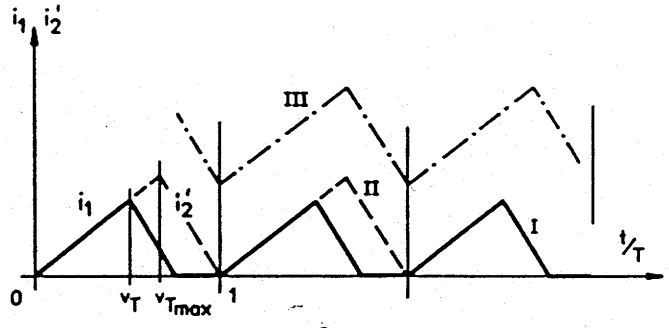

3a

Fig.3

a) Unidirectional converter
 I : discontinuous current
 II : intermediate case
 III: continuous current

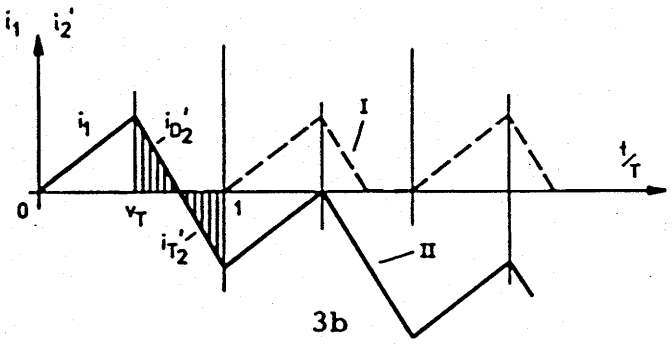

3b

b) Bidirectional converter
 I : discontinuous current (usually not used for bidirectional operation)
 II: continuous current

If one considers a practical realization of the circuit with FETs one has to note that T_2 (T_1) conducts part of the current besides D_2 (D_1); this is due to the gate signal (push-pull control) being present also for positive i_2 (negative i_1); the current distribution corresponds to the parallel circuit of turn-on resistance and nonlinear diode characteristic.

Since low voltage MOSFETs have very low R_{DSon} (some 10 mΩ) the current almost exclusively is conducted by the FET. This naturally also leads to low conduction losses. A further advantage of controlling (gating) the switch is given by avoiding the considerable reduction of the maximum allowable value of du/dt of the transistor; this appears after the conduction of the internal inverse diode (collector-base diode of the parasitic bipolar transistor). One more advantage is given by avoiding the high reverse current peak typical for the blocking behavior of the integrated diode. Only for high inverse currents in the pentode working region of the FET and due to the positive temperature coefficient of the turn-on resistance the diode characteristic will largely determine the behavior.

High voltage FETs show higher on-resistances (in the order of

magnitude of 1 Ω) due to the on-resistance increasing with the power of 2.5 dependent on the blocking voltage. A modification of the antiparallel diode characteristic therefore is only given for the lower current region. In connection with the previous remarks it seems advantageous therefore to block the internal inverse diode by a Schottky diode in series and to add a fast diode externally.

Concerning efficiency of the described system one has to note critically that, as mentioned, for no (low) load condition the energy oscillates between input and output. This leads to a considerable deterioration of the efficiency in connection with the nonideal behavior of the system components. The resistive losses appearing thereby can be reduced by reduction of the current ripple (increase of the effective inductances, increased size and volume, stray inductances). Further losses are due to magnetizing and demagnetizing the transformer core with switching frequency, which is largely load independent, however. This appears for each turn off as energy converted into heat being proportional to the sum of the stray inductances and the square of the current ripple maximum; thereby one also has to consider that the blocking voltage across the semiconductor switch is formed by the sum of supply voltage plus the transformed secondary voltage plus the voltage across the stray inductance.

3. MODEL REPRESENTATION OF THE BIDIRECTIONAL CONVERTER

For the derivation of the model equations for the bidirectional converter compare [1].

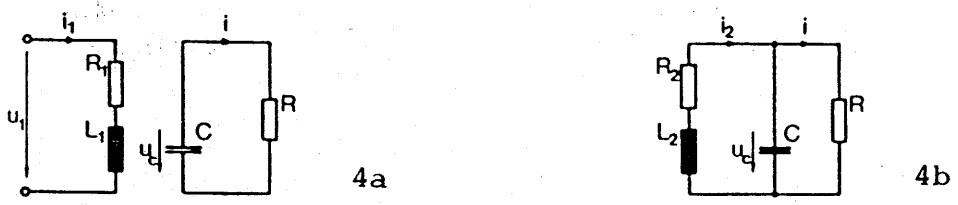

Fig.4 Equivalent circuit of the converter
a) turn-on switching state
b) turn-off switching state

Parasitic elements considered are the (ohmic) resistances on the primary and secondary R_1, R_2 (consisting of the sums of the winding resistances and the R_{Dson} of the semiconductor switches). During the interval t_{on} the equivalent circuit of Fig.4a is valid, leading to the equations

$$\frac{d(u_c)}{dt} = -\frac{u_c}{C \cdot R} \quad , \tag{1}$$

$$\frac{d(i_1)}{dt} = \frac{U_1}{L_1} - \frac{R_1}{L_1} \cdot i_1 \quad . \tag{2}$$

During the interval t_{off} the equivalent circuit of Fig.4b is applicable; the corresponding equations are

$$\frac{d(u_c)}{dt} = -\frac{u_c}{C \cdot R} + \frac{N_1}{C \cdot N_2} \cdot i_1 \quad , \tag{3}$$

$$\frac{d(i_1)}{dt} = -\frac{N_2}{N_1} \cdot \frac{u_c}{L_2} - i_1 \cdot \frac{R_2}{L_2} \quad . \tag{4}$$

These two sets of equations therefore describe the system behavior. Under the condition that the system time constants are large compared to the switching period we can combine these two sets of equations. The duty ratio shall be defined as

$$\alpha = V_T = \frac{t_{on}}{T} \quad . \tag{5}$$

Weighed by this duty ratio, the combination of the two sets yields

$$\frac{d(u_c)}{dt} = -\frac{u_c}{C \cdot R} + (1-\alpha) \cdot \frac{N_1}{C \cdot N_2} \cdot i_1 \quad , \tag{6}$$

$$\frac{d(i_1)}{dt} = -(1-\alpha) \cdot \frac{N_2}{N_1} \cdot \frac{u_c}{L_2} - i_1 \cdot \left[\frac{R_1}{L_1} \cdot \alpha + (\alpha-1) \cdot \frac{R_2}{L_2} \right] + \alpha \cdot \frac{u_1}{N_1} \quad . \tag{7}$$

The set of equations is transformed into a linearized system around the operating point by introducing

$$u_c = U_{co} + \hat{u}_c \,,$$
$$i_1 = I_{1o} + \hat{i}_1 \,, \qquad (8)$$
$$\alpha = \alpha_o + \hat{\alpha}$$

$$\begin{bmatrix} \frac{d(\hat{u}_c)}{dt} \\ \frac{d(\hat{i}_1)}{dt} \end{bmatrix} = \begin{bmatrix} A_{11} & A_{12} \\ A_{21} & A_{22} \end{bmatrix} \cdot \begin{bmatrix} \hat{u}_c \\ \hat{i}_1 \end{bmatrix} + \begin{bmatrix} B_{11} \\ B_{21} \end{bmatrix} \cdot \alpha \qquad (9)$$

with

$$A_{11} = -\frac{1}{R_o \cdot C} \,, \qquad A_{12} = (1-\alpha_o) \cdot \frac{-N_2}{C \cdot L_2 \cdot N_1} \,,$$

$$A_{21} = -\frac{1-\alpha_o}{L_2} \cdot \frac{N_2}{N_1} \,, \quad A_{22} = -\left[\alpha_o \cdot \frac{R_1}{L_1} + (1-\alpha_o) \cdot \frac{R_2}{L_2} \right], \qquad (10)$$

$$B_{11} = -\frac{I_{1o} \cdot N_1}{C \cdot N_2} \,, \quad B_{21} = \frac{U_{1o}}{L_1} + \frac{U_{co} \cdot N_2}{L_2 \cdot N_1} + \left[\frac{R_2}{L_2} - \frac{R_1}{L_1} \right] \cdot I_{1o} \,.$$

This leads to the following structure diagram Fig.6.

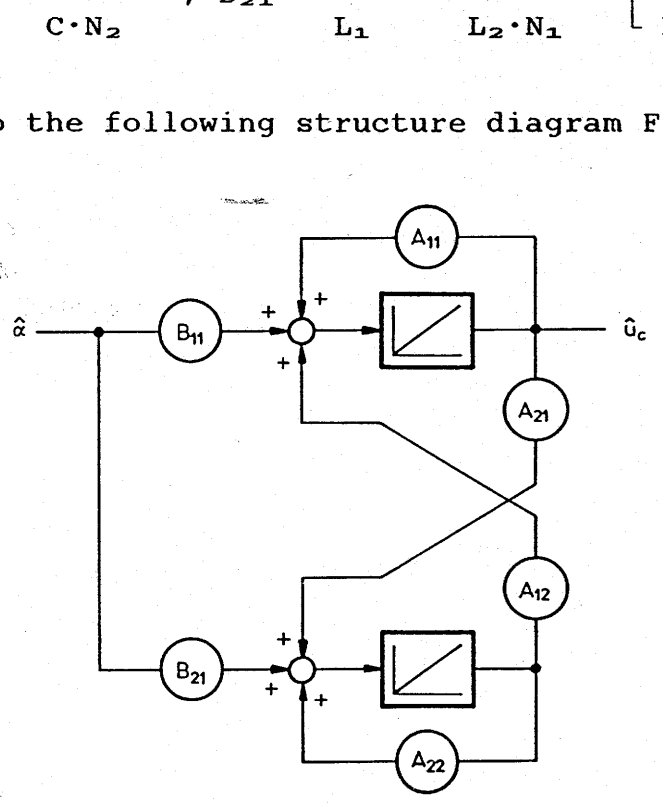

Fig.6 Structure diagram of the linearized bidirectional push-pull converter

The relationship for the stationary case results from:

$$\frac{1}{C}\cdot\frac{N_1}{N_2}\cdot I_{1o}\cdot(1-\alpha_o) - \frac{U_{co}}{R\cdot C} = 0 \qquad (11)$$

$$\frac{R_2}{L_2}\cdot(\alpha_o-1)\cdot I_{1o} + \frac{N_2}{N_1\cdot L_2}\cdot(\alpha_o-1)\cdot U_{co} + (U_{1o}+R_1\cdot\alpha_o)\cdot\frac{I_{1o}}{L_1} \qquad (12)$$

In the operating point (given by U_{1o},U_{co},I_{1o} and α_o) we can calculate from Eq.(9) the transfer function between output voltage u_{co} and the duty ratio α_o.

We receive

$$\hat{u}_c(s) = G_{u\alpha}(s)\cdot\hat{\alpha}(s) \qquad (13)$$

with

$$G_{u\alpha}(s) = \frac{s\cdot B_{11} + A_{12}\cdot B_{21} - A_{22}\cdot B_{11}}{s^2 - s\cdot(A_{11}+A_{22}) + \det(A)} \qquad (14)$$

4. THE BIDIRECTIONAL CONVERTER WITH CLOSED LOOP CONTROL

By linearization in the operating point the system of nonlinear equations (Eqs. 6,7) has been transformed into a linear one (Eq.9). Therefore it has been possible to give a transfer function of the bidirectional converter (Eq.14). Now it is possible to use the means of controller dimensioning for linear systems. One has to keep in mind, however, that the controller based on the dimensioning really works as designed only in the chosen operating point.

4.1 Pole-Zero-Diagram

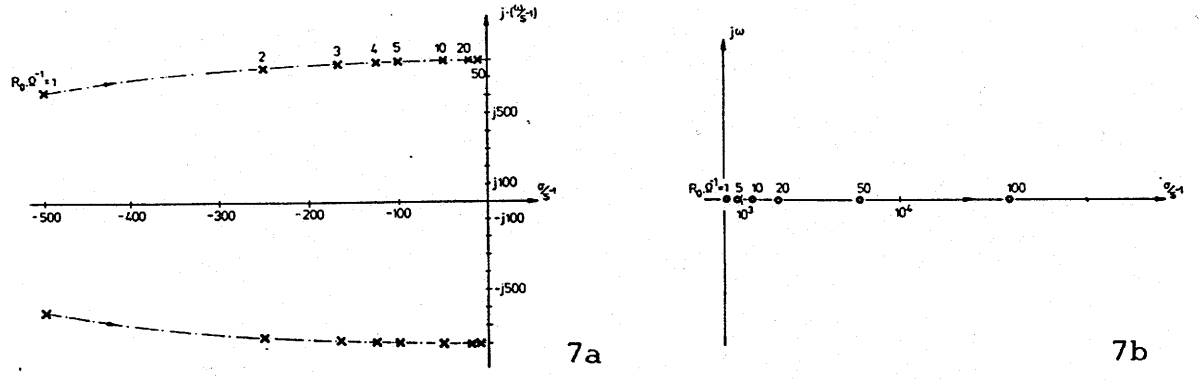

7a 7b

Fig.7 a) Pole locations for a bidirectional converter.
b) Zero location for a bidirectional converter.

In order to cover the operating behavior for varying operating points on has to determine pole-zero-diagrams for a representative number of different operating points. Fig. 7a shows the pole locations for a small experimental converter in dependency on the load. For lower load the poles come closer to the vertical axis and therefore the system becomes less damped. Fig. 7b shows the location of the zero for the same converter. The zero always lies in the right half plane and moves to the right for reduced load.

4.2 Bode Plot of the Controlled System

Fig. 8a and b show the Bode plot of the bidirectional converter for two different load conditions. Now one can base the controller dimensioning on the Bode plot [3,pp.168-207]. This results in a PI(proportional-integral)controller of the form

$$G_{PI1}(s) = 0.02 \cdot \left(1 + \frac{1}{1.67 \cdot 10^{-3} \cdot s}\right) \qquad (R_o = 1\Omega) \qquad (15)$$

and

$$G_{PI2}(s) = 3.2 \cdot 10^{-3} \cdot \left(1 + \frac{1}{1.6 \cdot 10^{-3} \cdot s}\right) \qquad (R_o = 10\Omega) \qquad (16)$$

One can see that the controller gain is dependent very much on the converter load. On the other hand, the integration time constant remains almost constant. The Bode plots for the open control loop are shown in Figs. 9a and b. An adaptive PI controller could comply with this property by changing the gain. However, if one does not want to afford an adaptive controller, this nonadaptive controller has to be dimensioned for the worst case. Here, this would be for the least damping of the controlled system.

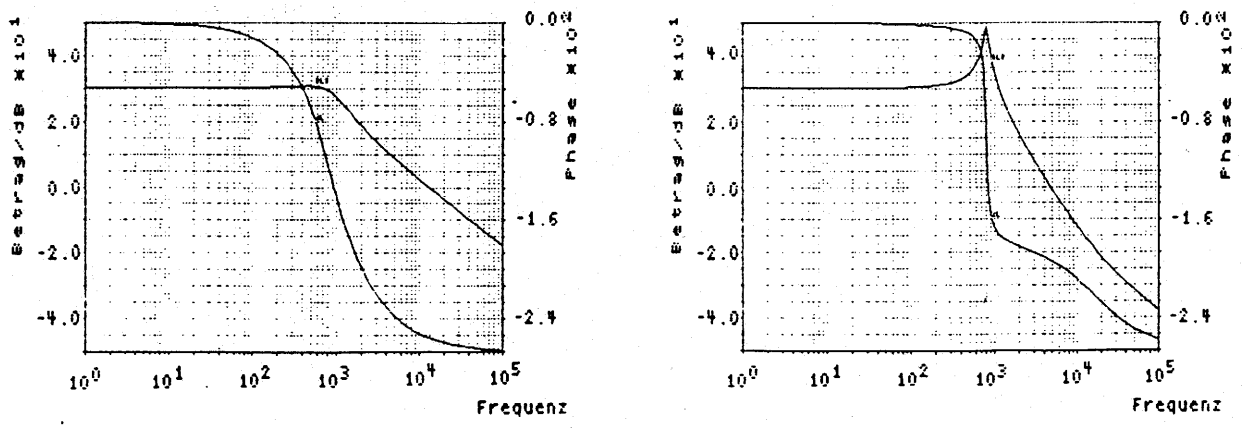

8a 8b

Fig.8 Bode plots for different loads of the bidirectional converter. a) $R_o = 1\Omega$, b) $R_o = 10\Omega$

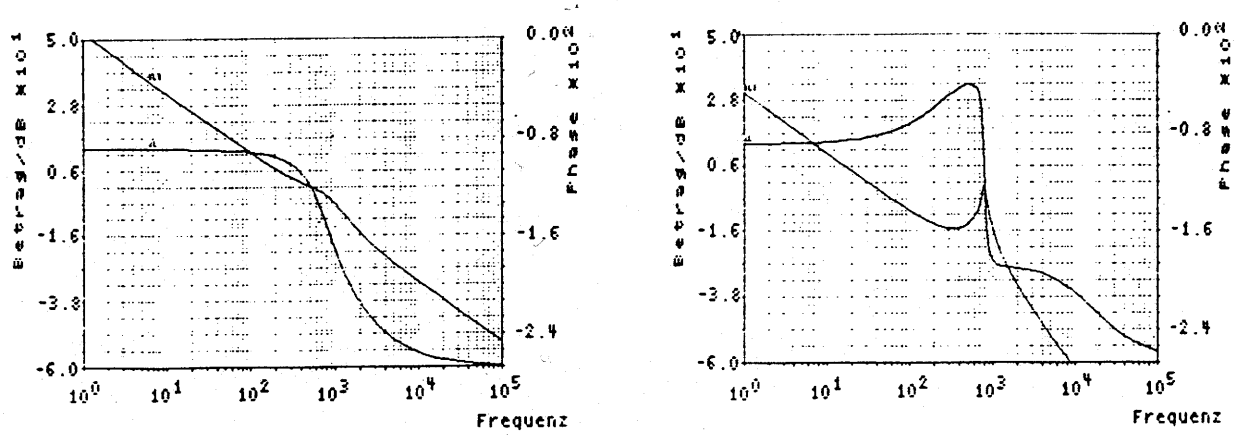

9a 9b

Fig.9 Bode plots for the open control loop
a)R_o=1Ω, b)R_o=10Ω

4.3 Bode Plot of the Closed Loop

The Bode plot (Fig.10a) shows the closed loop system behaviour for reference value changes (Fig.10b). However, for application as converter for constant output voltage the behaviour relative to load changes (disturbance frequency response) is decisive.

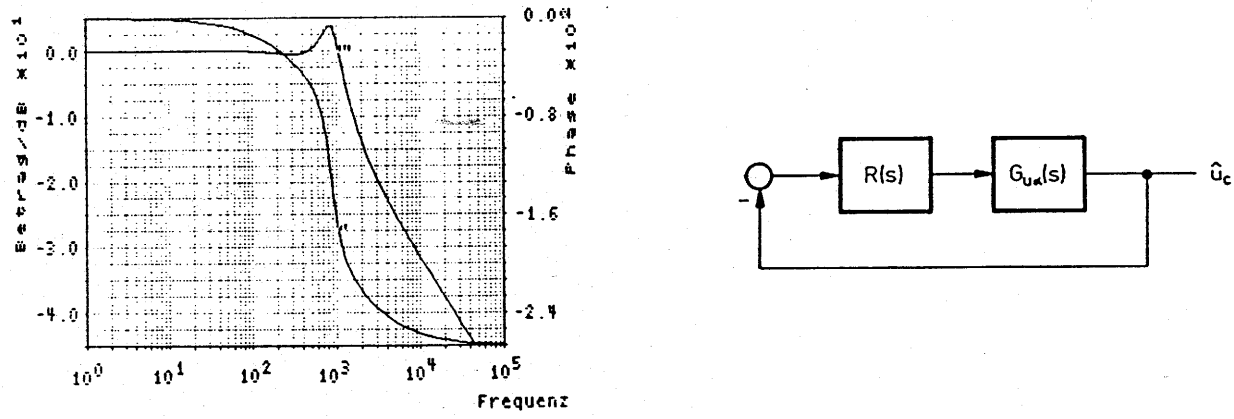

10a 10b

Fig.10 a) Bode plot for the closed loop
b) Functional block diagram

4.4 Root Locus

Besides the Bode plot the root locus diagram is well known as a second method for analysing and synthesis of linear control systems [3,p.149]. For the experimental converter considered here

the root locus is shown in Fig.11.

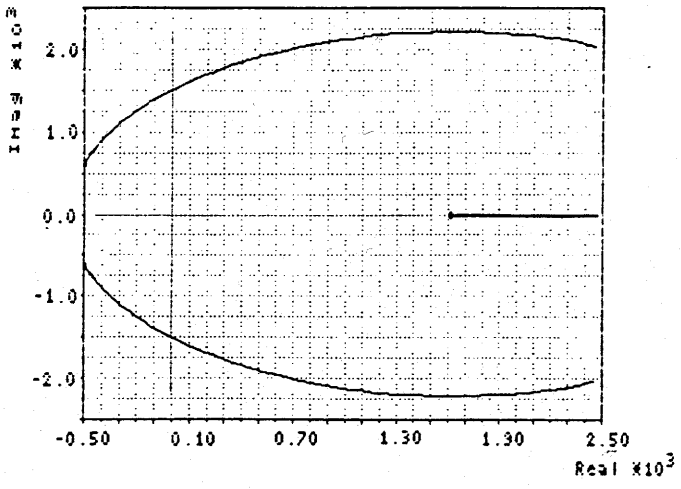

Fig.11 Root locus of a bidirectional converter

4.5 System Step Response

Fig. 12a shows the closed loop step response for controller 2 (Eq.16) as calculated based on the linearized system. Fig 12b shows the same closed loop step response for controller 2 (Eq.16), but calculated based on the nonlinear model (Eqs.6,7). One can notice the good consistency of the two results. Additionally it has to be mentioned that the system model has been simplified for the controller dimensioning by neglecting the winding resistance and the (differential) resistances of the power semiconductors. This means that the system in reality has a somewhat higher damping. This can be seen clearly from Fig. 12b.

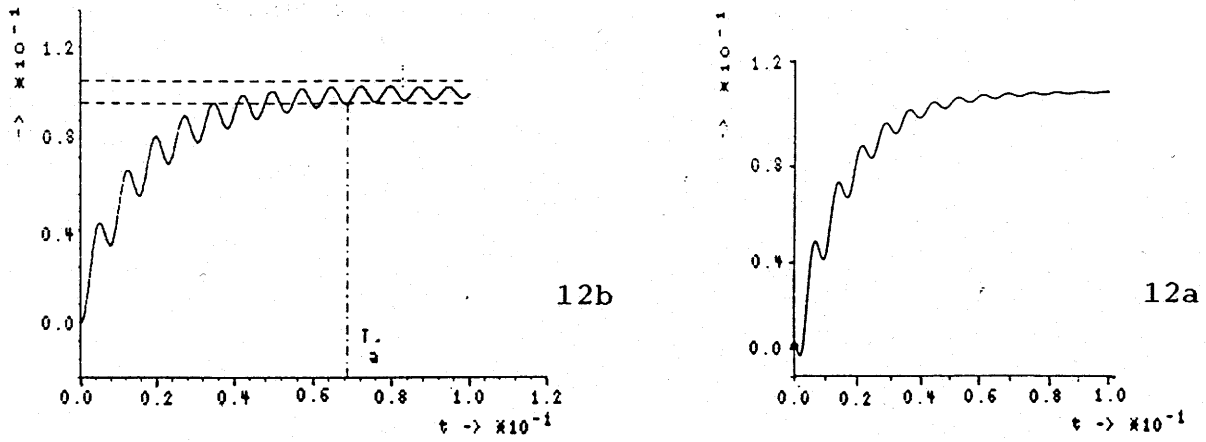

Fig.12 a)Closed loop response based on the linearized model
b)Closed loop response based on the nonlinear model

Finally the response to a disturbance input change (in our case a load change) shall be shown.

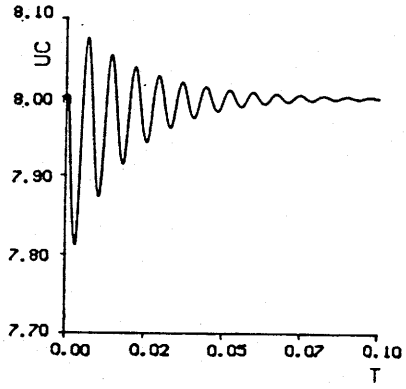

Fig.13 Response to a load change

5. CONCLUSIONS

A new system for DC-DC power conversion based on a buck-boost converter topology has been presented which makes power flow in both directions possible. This feature is useful for certain applications, such as UPS (uniterruptable power supplies). Closed loop control with a PI controller has been treated based on simulation using duty cycle averaging. The controller design has been shown for an example. By linearization in the operating point the system of nonlinear differential equations representing the bidirectional converter has been transformed in a linear one. Therefore it was possible to find a transfer function and so one can use the means of controller dimensioning for linear systems. The validity has been checked by comparison of the results of both model representations.

As the research shows closed loop control will require application of controllers of higher sophistication; due to the nonlinearity of the system its behavior varies in dependence of the operating point. An optimized controller therefore should be adaptive. This will be implemented in the near future.

REFERENCES

[1] Kolar,J.W.,Himmelstoss,F.A.,and Zach,F.C.:"Analysis of the control Behavior of a Bidirectional High-Frequency DC-DC-Converter", PCIM88,München 8.5.-10.5.1988,pp.344-359
[2] Middlebrook,R.D.,Cuk,S.:"Advances in Switched-Mode Power Conversion, Vol.1,Pasadena:Teslaco.1981
[3] Föllinger,O.:"Regelungstechnik",Heidelberg:Hüthig Verlag.1984

ACKNOWLEDGEMENT

The authors are very much indebted to the Austrian «Fonds zur Förderung der wissenschaftlichen Forschung» who supports the work of the power electronics section at their university.